Chemistry Europe
European Chemical Societies Publishing

Redox Chemistry of Heterobimetallic Polypnictogen Triple-Decker Complexes – Rearrangement, Fragmentation and Transfer

Martin Piesch,[a] Stephan Reichl,[a] Christoph Riesinger,[a] Michael Seidl,[a] Gabor Balazs,[a] and Manfred Scheer*[a]

Dedicated to Professor Andreas Hirsch on the occasion of his 60s birthday

Abstract: The redox chemistry of the heterobimetallic triple-decker complexes [(Cp*Fe)(Cp‴Co)(μ,η^5:η^4-E$_5$)] (E = P (**1**), As (**2**), Cp* = 1,2,3,4,5-pentamethyl-cyclopentadienyl, Cp‴ = 1,2,4-tri-tertbutyl-cyclopentadienyl) and [(Cp‴Co)(Cp‴Ni)(-μ,η^3:η^3-E$_3$)] (E = P (**10**), As (**11**)) was investigated. Compound **1** and **2** could be oxidized to the monocations **3** and **4** and further to the dications **5** and **6**, while the initially folded cyclo-E$_5$ ligand planarizes upon oxidation. The reduction leads to an opposite change in the geometry of the middle deck, which is now folded stronger into the direction of the other metal fragment (formation of monoanions **7** and **8**). For the arsenic compound **8**, a different behavior is found since a fragmentation into an As$_6$ (**9**) and As$_3$ ligand complex occurs. The Co and Ni triple-decker complexes **10** and **11** can be oxidized initially to the heterometallic monocations **12** and **13**, which are not stable in solution and convert selectively into the homometallic nickel complexes **14** and **15** and the cobalt complexes **16** and **17**. This behavior was further proven by the oxidation of [(Cp‴Co)(Cp″Ni)(μ,η^3:η^2-P$_3$)] (**19**, Cp″ = 1,3-di-tertbutyl-cyclopentadienyl) comprising two different Cp ligands. The transfer of {Cp^{R}M} fragments can be suppressed when a {W(CO)$_5$} unit is coordinated to the P$_3$ ligand (**20**) prior to the oxidation and the mixed cobalt and nickel cation **21** can be isolated. The reduction of **10** and **11** yields the heterometallic monoanions **22** and **23**, where no transfer of the {Cp^{R}M} fragments is observed.

Introduction

Elemental modifications of sulfur, phosphorus or arsenic can be reduced leading to a degradation under bond cleavage to yield S_6^{2-}, P^{3-} or As^{3-}, respectively.[1] On the other hand, oxidation reactions can cause the formation of new element-element bonds. While for the oxidation of S_8 to S_8^{2+} a novel S–S bond is formed, the oxidation of white phosphorus (P_4) is accompanied by an aggregation to form P_9^+.[2] A similar reactivity can be observed for cyclic phosphines or arsines such as $^tBu_4E_4$ (E = P, As). Both can be reduced by degradation to $^tBu_2E_2^{2-}$ using for example elemental potassium.[3] On the other hand, organometallic complexes such as ferrocene reveal a versatile redox chemistry. The parent ferrocene has played an important role in recent research,[4] not only as the redox couple [Cp$_2$Fe]/[Cp$_2$Fe]$^+$, which is widely used as a reference system for electrochemical investigation methods such as cyclic voltammetry.[5] Moreover, ferrocene-containing fragments are commonly used as molecular switches in redox switchable catalysis (RSC).[6] For some systems, more redox states are needed and therefore more than one ferrocene unit was incorporated e.g. in macrocycles.[7] According to the isolobal relationship between CH and P or As, the CH units in C_5H_5 ligand can partially be replaced by pnictogen atoms revealing ligands as for instance phospholes (C_4H_4P, $C_2H_2P_3$)[8,9,10] or arsoles (C_4H_4As, $C_2H_2As_3$),[8,10,11] or *cyclo*-E$_5$ (polypnictogen) ligands as for instance in the pentaphospha- and pentaarsaferrocene [Cp*Fe-(η^5-E$_5$)] (E = P, As).[12,13] The latter reveal a distinct redox chemistry,[14] however, most of these processes are irreversible and proceed via dimerization and fragmentation processes. A similar behavior was observed for the sandwich complexes [Cp‴Co(η^4-P$_4$)][15] and [(Cp‴Ni(η^3-P$_3$)][16] and the tetrahedrane compound [{CpMo(CO)$_2$}$_2$(μ,η^2:η^2-E$_2$)][17] (E = P, As, Sb, Bi). These complexes respond to redox reactions with either dimerization (e.g. to [(Cp‴Co)$_2$(μ,η^3:η^3-P$_8$)]$^{2-}$(**A**), Scheme 1) or a fragmentation and rearrangement takes places (e.g. to [(Cp‴Ni)$_2$(μ,η^2:η^2-P$_8$)]$^{2-}$ (**B**), Scheme 1).

On the other hand, going from sandwich complexes to homometallic polypnictogen triple-decker complexes, a fully reversible redox chemistry over two oxidation states as e.g. in

[a] Dr. M. Piesch, S. Reichl, C. Riesinger, Dr. M. Seidl, Dr. G. Balazs, Prof. Dr. M. Scheer
Institut für Anorganische Chemie
Universität Regensburg
93040 Regensburg (Germany)
E-mail: manfred.scheer@ur.de
Homepage: https://www.uni-regensburg.de/chemie-pharmazie/anorganische-chemie-scheer/

Supporting information for this article is available on the WWW under https://doi.org/10.1002/chem.202100844

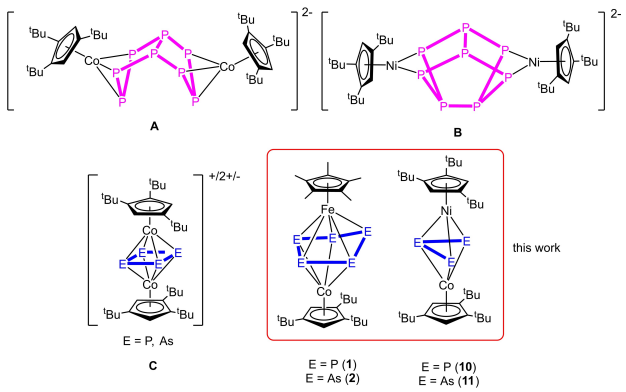

Scheme 1. Selected examples of oxidized and reduced polypnictogen ligand complexes heterobimetallic triple-decker complexes [(Cp*Fe)(Cp‴Co)(μ,η^5:η^4-E$_5$)] (E = P (**1**), As (**2**)) and [(Cp‴Co)(Cp‴Ni)(μ,η^3:η^3-E$_3$)] (E = P (**10**), As (**11**)).

[(Cp^{R}Mo)$_2$(μ,η^6:η^6-E$_6$)] (E = P, As)[18] or even over four and five redox stages takes place, which was found for the cobalt complex [(Cp‴Co)$_2$(μ,η^2:η^2-E$_2$)] (E = P, As).[19] Oxidation and reduction of the latter two induce a cyclization of the initially separated E$_2$ units to form a *cyclo*-E$_4$ ligand in [(Cp‴Co)$_2$(μ,η^4:η^4-E$_4$)]$^{+/2+/-}$ (**C**, Scheme 1).

Intrigued by the diversity of the structural changes and/or rearrangement processes upon oxidation and/or reduction of the homometallic polypnictogen ligand complexes, we were interested in investigating how the heterobimetallic polypnictogen triple-decker complexes would respond to the withdrawal or addition of electrons. Would a simple rearrangement of the E$_n$ ligand, a release of a {Cp^{R}M} fragment and/or an aggregation to larger polypnictogen ligands take place to form multimetallic cluster complexes? Would the redox processes be reversible and would there be a difference between phosphorus- and arsenic-containing derivatives, considering the in general lower E–E bond energy for arsenic? Therefore, we were intrigued to investigate the redox chemistry of the mixed iron/cobalt triple-decker complexes [(Cp*Fe)(Cp‴Co)(μ,η^5:η^4-E$_5$)] (E = P (**1**), As (**2**)) and the mixed cobalt/nickel triple-decker complexes [(Cp‴Co)(Cp‴Ni)(μ,η^3:η^3-E$_3$)] (E = P (**10**), As (**11**) to explore the response of these complex systems within the redox behavior.

Results and Discussion

The heterobimetallic triple-decker complexes [(Cp*Fe)(Cp‴Co)(-μ,η^5:η^4-E$_5$)] (E = P (**1**), As (**2**)) can be easily synthesized by the reaction of the cobalt toluene complex [(Cp‴Co)$_2$(μ,η^4:η^4-C$_7$H$_8$)] with [Cp*Fe(η^5-E$_5$)] (E = P, As)] in gram scale.[20,21] To obtain a first overview if redox processes are accessible, cyclic voltammetry measurements were performed revealing several redox processes (cf. Supporting Information). Both compounds can be oxidized using one equivalent of the Ag(I) salt containing the weakly coordinating anion [FAl]$^-$ ([FAl{OC$_6$F$_{10}$(C$_6$F$_5$)}$_3$]$^-$) leading to the isostructural compounds [(Cp*Fe)(Cp‴Co)(μ,η^5:η^5-E$_5$)][FAl] (E = P (**3**), As (**4**)) which can be isolated in crystalline yields of 55 and 63 %, respectively (Scheme 2). Compound **3** can be obtained as green, **4** as brown air- and moisture-sensitive solids. Crystals suitable for single crystal X-ray structure analysis were obtained from concentrated solutions in CH_2Cl_2 layered with hexane at -30 °C. The structures in the solid state (Figure 1) reveal dinuclear triple-decker complexes with a slightly folded *cyclo*-E$_5$ ligand as middle deck while the ligand planarized compared to the starting materials. The E$_5$ ligand coordinates to both iron and cobalt fragments in an η^5 fashion, while E1 is bent out of the plane (fold angle E2-E4-E5-E1) by approx. 9.4° (**3**) and 13.6° (**4**), respectively (35.0° in **1**, 37.9° in **2**). All E–E bonds are shortened compared to **1** and **2**. For **3**, very similar P-P distances between 2.1214(9) and 2.1601(9) Å are present, while **1** shows three shorter distances (P1-P2 2.1459(10) Å, P3-P4 2.1283(10) Å, P1-P5 2.1498(10) Å) and two longer ones (P2-P3 2.2244(11) Å, P4-P5 2.2407(10) Å). For the analog arsenic compound **4**, the situation is similar. All As–As distances are in the range between 2.3224(8) and 2.3619(8) Å and shortened compared to **2**, while in **2**, three shorter distances (As1-As2 2.3682(5) Å, As3-As4 2.3401(5) Å, As1-As5 2.3716(6) Å) and two longer ones (As2-As3 2.4627(5) Å, As4-As5 2.4383(6) Å) are present. Compounds **3** and **4** are paramagnetic. The ^{1}H NMR spectrum of **3** in CD_2Cl_2 reveals four strongly broadened and shifted signals centered at δ = 5.66, 3.76, 3.29 and −65.22 ppm with an integral ratio of 15:9:18:2, while the signal at 5.66 ppm can be assigned to the Cp* ligand, and the other three singlets correspond to the Cp‴ ligand. The ^{31}P{^{1}H} NMR spectrum shows one broad singlet at δ = 275.1 ppm. The ^{1}H NMR spectrum of **4** in CD_2Cl_2 reveals three strongly broadened and shifted signals centered at δ = 3.84, 2.74 and −1.09 ppm with an integral ratio of 9:18:15, while the signals at 3.84 and

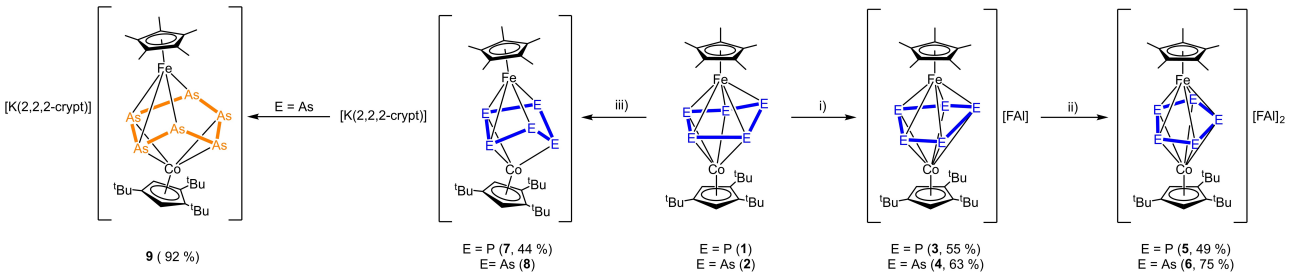

Scheme 2. Reaction of [(Cp*Fe)(Cp‴Co)(μ,η^5:η^4-E$_5$)] (E = P (**1**), As (**2**)) with: i) Ag[FAl] in CH_2Cl_2 at room temperature; ii) Ag[FAl] in *o*-$C_6H_4F_2$ at room temperature and iii) KC_8 in the presence of 2,2,2-crpytand in dme.

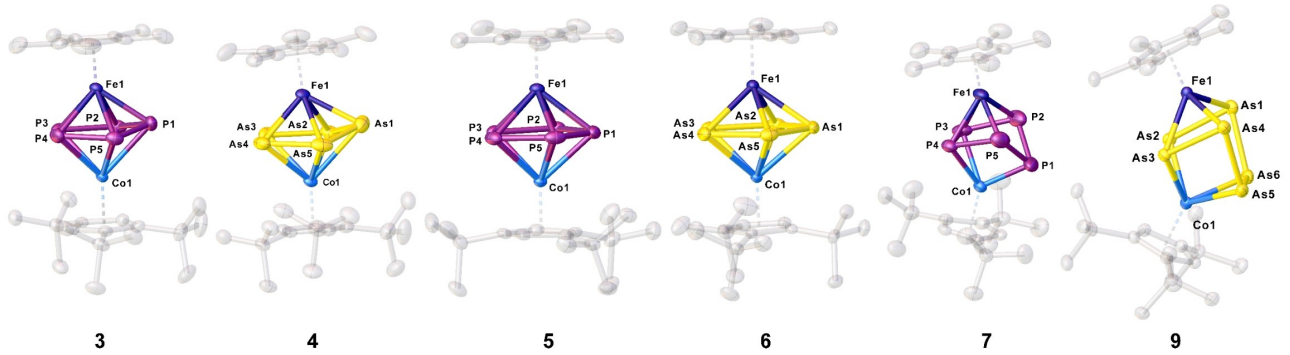

Figure 1. Molecular structures of **3–7** and **9** in the solid state. Thermal ellipsoids are drawn with 50% probability level. Hydrogen atoms, solvent molecules, anions and cations, respectively, are omitted for clarity.

2.74 ppm can be assigned to the ^{t}Bu groups of the Cp‴ ligands and the singlet at −1.09 ppm of the Cp* ligand. No signal for the C–H groups of the Cp‴ ligand can be detected between +125 and −125 ppm. The Evans NMR spectrum shows an effective magnetic moment of 2.04 μ_B for **3** and 1.90 μ_B for **4** corresponding to about one unpaired electron each. The EPR spectrum of **3** at 77 K (frozen *o*-$C_6H_4F_2$ solution) exhibits a strong rhombic resonance with hyperfine coupling to Co (g_1 = 2.155, g_2 = 2.035, g_3 = 1.948, A_1^{Co} = 290, A_2^{Co} = 55, A_3^{Co} = 120 MHz, Figure 2). DFT calculations reveal that the spin density is mainly located on the Co1 atom with some minor participation of P1 and Fe1 (cf. Figure 2) For **4**, the EPR spectra reveal rhombic resonances similar to those of **3**. The calculations show that the spin density is more equally distributed over Fe, Co and As1 and, compared to **3**, the signal is more asymmetric with the *g* values being more different (77 K, solid: g_1 = 2.235, g_2 = 1.952, g_3 = 1.896, Figure 2). The presence of the hyperfine coupling in the EPR spectrum of **3** and the pronounced rhombic signal in **4** indicates a rather metal centered oxidation.

Using two equivalents of Ag[FAl] in the oxidation of **1** and **2**, respectively, gives the dicationic compounds [(Cp*Fe)(Cp‴-Co)(μ,η^5:η^5-E_5)][FAl]$_2$ (E = P (**5**), As (**6**)) in crystalline yields of 49 and 75%, respectively (Scheme 2). Both compounds can be obtained as air- and moisture-sensitive brown solids. Crystals suitable for X-ray single crystal structure analysis were obtained from concentrated solutions in *o*-$C_6H_4F_2$ layered with hexane (**5**) and toluene (**6**) and stored at −30 °C, respectively. The structures in the solid state (Figure 1) reveal dinuclear triple-decker complexes with a planar *cyclo*-E_5 ligand as middle deck. In the compounds **5** and **6**, the *cyclo*-E_5 ligand coordinates to both the iron and cobalt fragments in an η^5 fashion and is planar, while it is slightly folded in the monocations **3** and **4** or strongly folded in the related starting materials **1** and **2**. For **5**, all P-P distances are between 2.1425(16) and 2.1521(16) Å and are in the range between P-P single and double bonds.[22,23] They are only slightly longer than in [Cp*Fe(η^5-P_5)] showing distances in the range of 2.1158(15) and 2.1268(16) Å.[24] For **6**, the As–As distances are in the range of 2.3390(6) and 2.3515(8) Å and also between single and double bonds.[22,23] Compared to [Cp*Fe(η^5-As_5)] the As–As bonds are only slightly elongated (2.317(1)–2.330(1) Å).[25] Interestingly, the diamagnetic dicationic compounds **5** and **6** are isostructural and isoelectronic to the monocationic homo- and heterobimetallic complexes [(Cp^{R}M)(Cp$^{R'}$M′)(μ,η^5:η^5-E_5)]$^+$ (M = Fe, Ru, M′ = Fe, Ru, E = P, As).[12,26] The ^{1}H NMR spectrum of **5** in *o*-$C_6H_4F_2$ with C_6D_6 capillary shows four singlets centered at δ = 3.69, 1.49, 1.39 and 1.21 ppm with an integral ratio of 2:18:9:15. In the ^{31}P{^{1}H} spectrum of **5**, a sharp singlet at δ = 52.7 ppm is monitored. In the ^{1}H NMR spectrum of **6**, four singlets centered at δ = 4.20, 1.25, 1.18 and 0.86 ppm with an integral ratio of 2:18:9:15 are detected.

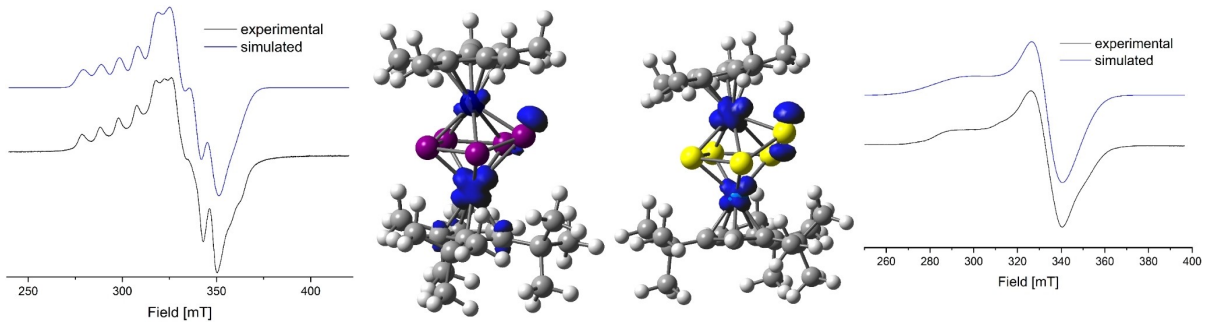

Figure 2. Experimental (black) and simulated (blue) X-band EPR spectra of **3** (left) and **4** (right) in frozen *o*-$C_6H_4F_2$ solution and the iso-surfaces of the calculated spin density (BP86/def2-TZVP level of theory) in **3** (left middle) and **4** (right middle).

Therefore, the oxidation of **1** and **2** leads to a successive planarization of the folded *cyclo*-E_5 ligand resulting in a completely planar ligand in **5** and **6**, which is accompanied by an overall significant shortening of all E-E distances. All oxidation reactions are fully reversible upon addition of KC_8.

The question arises how **1** and **2** will respond to a chemical reduction. Compound **1** can be reduced using potassium graphite in the presence of 2,2,2-cryptand to give [K(2,2,2-crypt][(Cp*Fe)(Cp‴Co)(μ,η^4:η^3-P_5)] (**7**) in crystalline yields of 44% (Scheme 2). Compound **7** can be isolated as an extremely air- and moisture-sensitive dark green solid. Crystals of **7** suitable for single crystal X-ray structure analysis were obtained from a concentrated solution in thf layered with hexane at −30 °C. The structure of **7** in the solid state (Figure 1) reveals a dinuclear triple-decker complex with a strongly folded *cyclo*-P_5 middle deck. The P_5 ligand coordinates to the iron fragment in an η^4 and to the cobalt fragment in an η^3 fashion. One P atom (P1) is bent out of the plane by approx. 44.5°. All P-P distances are in the range of single bonds. Compound **7** is paramagnetic. The ^{1}H NMR spectrum in thf-d_8 shows three broad and strongly shifted signals for the ^{t}Bu and Me groups of the Cp ligands, while no signal for the H atoms directly attached to the Cp‴ ligand can be detected. The effective magnetic moment was determined to be 2.01 μ_B by the Evans method corresponding to about one unpaired electron. The EPR spectrum shows an isotropic resonance with *g* values near to 2.0 indicating one unpaired electron (293 K, solid, g_{iso} = 2.060, cf. Supporting Information), while the spectra of **3** and **4** show rhombic resonances.

The folding of the *cyclo*-P_5 ligand in **1** is clearly dependent on the oxidation state. The oxidation to the mono cation **3** and the dication **5** leads to a successive planarization of the P_5 ligand, while the reduction inverts the folding and the P1 atom turns from the coordination to Fe1 to Co1 accompanied by an increase of the folding angle. For the reduction of the arsenic complex **2**, potassium graphite in the presence of 2,2,2-cryptand was used (Scheme 2). Regardless of numerous attempts, it was not possible to obtain crystals of the analog arsenic complex [K(2,2,2-crypt)][(Cp*Fe)(Cp‴Co)(μ,η^4:η^3-As_5)] (**8**) yielding always only brown oily residues. But the presence of **8** was proved by paramagnetic signals in the ^{1}H NMR spectrum of the reaction mixture (mixture of **8**, **9** and unknown compound, cf. Supporting Information) and a strong isotropic resonance in the EPR spectra of the precipitated solid of the reaction mixture with *g* values near to 2 (77 K, solid: g_{iso} = 2.123, r.t, solid: g_{iso} = 2.109). Leaving the Schlenk flasks with the oily residues of the crystallization at room temperature for a few weeks, a large amount of crystalline [K(2,2,2-crypt)][(Cp*Fe)(Cp‴Co)(μ,η^4:η^4-As_6)] (**9**) could be obtained in isolated yields of 92% (Scheme 2). The formation of **9** is reproducible. The ^{1}H NMR spectrum of the mother liquor reveals [(Cp*Fe)(Cp‴Co)(μ,η^3:η^3-As_3)] as a side product.[21] The solid-state structure of **9** is shown in Figure 1. The molecular structure reveals a dinuclear triple-decker complex with a newly formed bent *cyclo*-As_6 ligand as middle deck. All As–As bonds except As2-As3 are in the range of single bonds (2.3441(5)–2.4420(5) Å). The As2-As3 distance of 2.6907(5) Å displays a strongly elongated As–As single bond indicated by a WBI of 0.52.[23] The structural motif of **9** is reminiscent of the isoelectronic cobalt complex [(Cp$^+$Co)$_2$(μ,η^4:η^4-As_6)],[27] however, in **9** as heterobinuclear complex. The ^{1}H NMR spectrum of **9** in thf-d_8 shows four singlets centered at δ = 4.14, 1.61, 1.53 and 1.35 ppm with an integral ratio of 2:15:18:9.

While the reduction of **1** to **7** is fully reversible upon addition of $AgBF_4$, this is not the case for the arsenic derivate **2** due to the fragmentation of the As_5 ligand to yield **9**.

The second scope of this work was the investigation of the redox behavior of the mixed cobalt and nickel triple decker complexes [(Cp‴Co)(Cp‴Ni)(μ,η^3:η^3-E_3)] (E = P (**10**), As (**11**). Both compounds can be easily prepared from the reaction of [Cp‴Ni(η^3-E_3)] (E = P, As) with the cobalt toluene complex [(Cp‴Co)$_2$(μ,η^4:η^4-C_7H_8)] in gram scale. The synthesis of **10** was already reported[20] and the arsenic derivative **11** was prepared analogously (cf. experimental section). To obtain a first insight into possible redox processes of **10** and **11**, cyclic voltammetric measurements were conducted, which reveal several possible redox processes (cf. Supporting Information). The oxidation of **10** and **11** with one equivalent Ag[FAl] leads to a color change of dark brown to red-brown within one hour (**10**) and to an immediate color change from dark green to brown (**11**), respectively. The ^{1}H NMR spectra in CD_2Cl_2 of both reaction mixtures after one hour reveal the formation of paramagnetic species, which is in agreement with the abstraction of one electron by the oxidation. Stirring the mixtures overnight and recording another ^{1}H NMR spectrum after one day shows the formation of two new diamagnetic species each while the initial paramagnetic compounds have disappeared completely. In the ^{31}P{^{1}H} NMR spectrum of the reaction mixture of **10** with Ag[FAl] in CD_2Cl_2, no signals could be detected after one hour, but, after one day, a broad singlet centered at δ = 140.2 ppm and a set of a doublet (δ = 789.0 ppm) and a triplet (δ = −218.0 ppm) with a $^1J_{PP}$ coupling constant of 361 Hz and an integral ratio of 2:1 could be observed. The first species could be identified as [(Cp‴Ni)$_2$(μ,η^3:η^3-P_3)][FAl] (**14**) (cf. Scheme 3), which had already been reported, however with $[GaCl_4]^-$ as a counterion.[28] The mixtures from the reaction of **10** and **11** with Ag[FAl], respectively, were layered with hexane and left at −30 °C for crystallization. After a few days, red blocks of [(Cp‴Co)$_2$(μ,η^3:η^3-P_3)][FAl] (**16**) and brown blocks of [(Cp‴Co)$_2$(μ,η^3:η^3-As_3)][FAl] (**17**) could be isolated in 65% and 17% yields, respectively (Scheme 3). The ^{1}H and ^{31}P{^{1}H} NMR spectra of the mother liquors show each an enrichment of the nickel complexes [(Cp‴Ni)$_2$(μ,η^3:η^3-P_3)][FAl] (**14**) and [(Cp‴Ni)$_2$(μ,η^3:η^3-As_3)][FAl] (**15**). The identity of **14** was proven by comparison with the NMR spectra of [(Cp‴Ni)$_2$(μ,η^3:η^3-P_3)][$GaCl_4$],[28] and analytically pure [(Cp‴Ni)$_2$(μ,η^3:η^3-As_3)][FAl] (**15**) could be obtained by the oxidation of [Cp‴Ni(η^3-As_3)] with [Fc^{Diac}][FAl] more selectively (cf. experimental section). Obviously, a strong tendency of a rearrangement to homometallic triple-decker complexes is present. Before these rearrangement processes take place, the oxidation of **10** and **11** to the heterometallic monocations [(Cp‴Co)(Cp‴Ni)(μ,η^3:η^3-E_3)][FAl] (E = P (**12**), As (**13**)) displays the first step. Compounds **12** and **13** could not be crystallized due to their further transformation to **14**/**16** and **15**/**17** in solution,

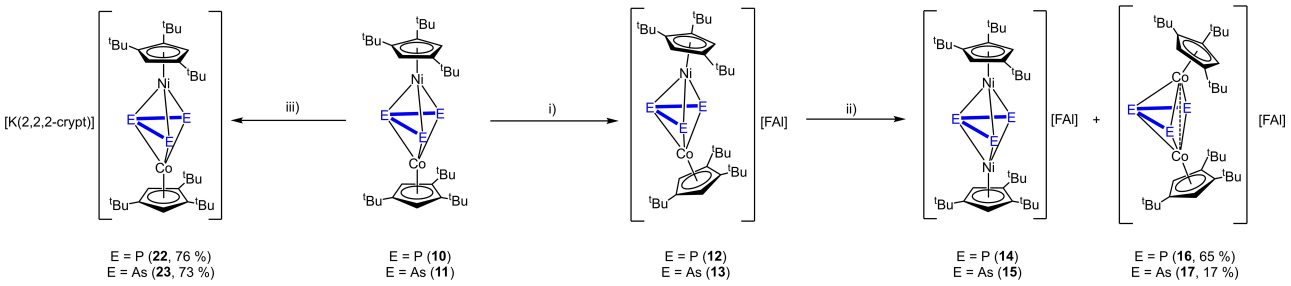

Scheme 3. Reaction of [(Cp‴Co)(Cp‴Ni)(μ,η^3:η^3-E_3)] (E = P (**10**), As (**11**) with i) Ag[FAl] in CH_2Cl_2, ii) leaving the reaction mixture at room temperature overnight and iii) potassium graphite in dme in the presence of 2,2,2-cryptand.

respectively (Scheme 3). But the reaction can be stopped by precipitation with hexane after a few minutes. The obtained solids contain **12** and **13** as major compounds (determined by NMR) and were further investigated by EPR spectroscopy. The X-band EPR spectrum of a freshly prepared CH_2Cl_2 solution (see Figure 3) of **12** at room temperature shows a rhombic resonance (g_1 = 2.023, g_2 = 2.031, g_3 = 2.014) with a well resolved hyperfine coupling to cobalt (A_1^{Co} = 60, A_2^{Co} = 64, A_3^{Co} = 63 MHz), indicating that the oxidation occurred on the metal centers. The EPR spectrum in frozen solution (77 K) shows one broad resonance while the coupling is not resolved (cf. Supporting Information). The solid compound **12** is EPR-silent at room temperature and 77 K. For the arsenic derivative **13**, a resonance can be detected for the solid and of the frozen CH_2Cl_2 solution only at 77 K. This resonance at 77 K shows a rhombic character (g_1 = 2.155, g_2 = 2.071, g_3 = 2.016) without any hyperfine couplings. Since the molecular structures could not be determined by XRD, DFT calculations (BP86/def2-TZVP level of theory) were performed starting either on the strongly bent geometry of the cobalt complexes **16**/**17** or from the more planar geometry of the nickel complexes **14**/**15**. The bent isomers **12-bent**/**13-bent** are energetically favored by 20.3 and 3.5 kJ/mol, respectively, compared to their linear isomers **12-linear**/**13-linear**. The spin density of both isomers differs significantly, being neither mainly located on the nickel atom (**12-bent**/**13-bent**) nor on the cobalt atom (**12-linear**/**13-linear**) (cf. Figure 3 and S83). In agreement with the EPR data of **12**, the linear isomer seems to be predominant in solution, albeit energetically slightly disfavored. In the case of the arsenic derivative **13**, the bent isomer seems to be predominant in frozen solution as well as in the solid state due to the absence of a hyperfine coupling to cobalt and the presence of a rhombic signal shape (the free electron is preferably located on a metal center). Since **12** and **13** could not be obtained as analytically pure compounds, no Evans NMR experiments were conducted. The further rearrangement of the heterometallic cation **12**/**13** to the homometallic nickel (**14**/**15**) and cobalt (**16**/**17**) cations is exothermic by 95.5 and 73.9 kJ/mol (related to **12-bent**/**13-bent**), respectively.

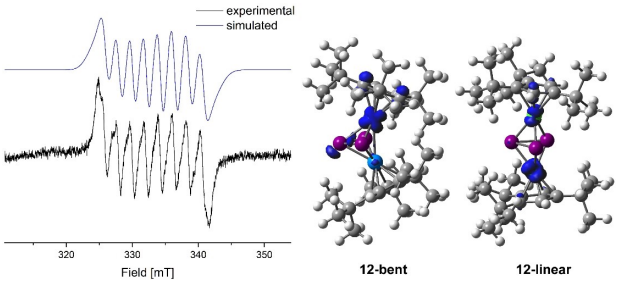

Figure 3. X-band EPR spectrum of **12** in CH_2Cl_2 at room temperature (experimental (black) and simulated (blue)) and the isosurfaces of the calculated spin densities in **12-bent** and **12-linear**.

As already mentioned, leaving the reaction mixtures of the oxidation experiments of **10** and **11** with Ag[FAl] for crystallization yields single crystals of [(Cp‴Co)$_2$(μ,η^3:η^3-E_3)][FAl] (E = P (**16**), As (**17**)) suitable for X-ray diffractions. The structures in the solid state are depicted in Figure 4. The molecular structure reveals a strongly bent triple-decker complex with an E_3 chain ligand coordinated to two {Cp‴Co} fragments. The E_3 ligand shows two short distances (P1-P2 2.1532(12) Å, P2-P3 2.1516(21) Å, As1-As2 2.3770(5) Å, As2-As3 2.3638(5) Å being in the range between single[23] and double[22] bonds, which is also in agreement with the calculated WBIs of 1.07/1.07 (**16**) and 1.02/1.02 (**17**). The outer E atoms E1 and E3 are 3.2571(11) Å (**16**) and 3.5176(6) Å (**17**) away from each other and clearly represent no bond (WBIs of 0.17 (**16**) and 0.17 (**17**)). The Co···Co distances of 2.6213(6) Å (**16**) and 2.6827(6) Å (**17**) are quite short and an interaction could not be dismissed, supported by the calculated WBIs of 0.18 (**16**) and 0.17 (**17**), respectively. Compound **13** and **15** are isoelectronic and isostructural to the starting materials **10** and **11**, while **17** is isoelectronic and isostructural to the mixed iron and cobalt complex [(Cp*Fe)(Cp‴Co)(μ,η^3:η^3-As_3)].[21] Single crystals of the nickel complexes [(Cp‴Ni)$_2$(μ,η^3:η^3-E_3)][FAl] (E = P (**14**), As (**15**)) as the second product were not obtained from these reaction mixtures. Since the phosphorus derivative was already reported,[28] only the so far unknown arsenic complex **15** will be discussed here. Single crystals of **15** were obtained from a concentrated solution of the reaction mixture of the oxidation of [Cp‴Ni(η^3-As_3)] with [Fc^{Diac}][FAl] in CH_2Cl_2 layered with pentane at room temperature. The structure in the solid state (Figure 4) shows a triple-decker complex with an As_3 ligand coordinated to two {Cp‴Ni} fragments. The As_3 ligand shows two shorter distance (As1-As2 2.4179(4) Å, As2-As3 2.4294(3) Å) and one long distance (As1-As3 2.8730(4) Å). The short distance

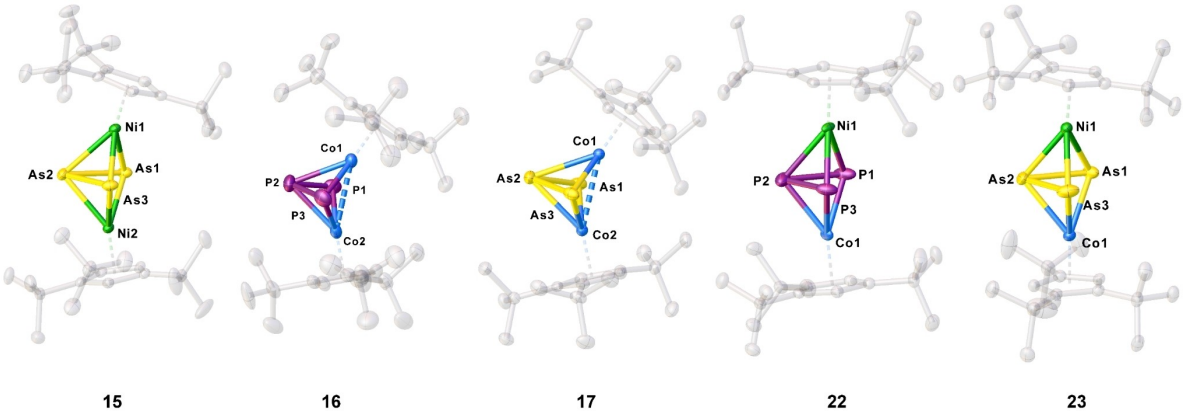

Figure 4. Molecular structures of **15**, **16**, **17**, **22** and **23** in the solid state. Thermal ellipsoids are drawn with 50% probability level. Hydrogen atoms, solvent molecules, anions and cations, respectively, are omitted for clarity.

is in the range between As–As single and double bonds (calculated WBIs of 1.02 and 1.03) and the long distance is too long to be considered as a bond, but since the distance is still below the sum of van der Waals radii,[29] a weak interaction could not be dismissed, which is underlined by the calculated WBI of 0.36. The Ni atoms are 3.5434(5) Å apart from each other, which is clearly too long for an interaction (WBI of 0.05).

To obtain further proof of the transfer of the {Cp‴M} fragments during the oxidation process, [(Cp‴Co)(Cp″Ni)(-μ,η^3:η^2-P$_3$)] (**18**) with two different Cp ligands was synthesized by the reaction of [Cp″Ni(η^3-P$_3$)] with [(Cp‴Co)$_2$(μ,η^4:η^4-C$_7$H$_8$)]. Interestingly, the change from Cp‴ to Cp″ leads to a significant change in the geometry of the heterometallic triple-decker complex in the solid state (Figure 5). Due to the lower steric demand of the Cp″ ligand, the geometry changes from a slightly bent triple-decker complex such as in **10** to a structural motif where the {Cp″Ni} fragment is almost in the plane of the P$_3$ ligand (torsion angle of only 7.5°).

This geometry is energetically favored by 33.5 kJ/mol towards the stretched triple-decker geometry observed for **10** (cf. Figure S86). In the ^{31}P{^{1}H} NMR spectrum of **18** in C$_6$D$_6$, only the bent isomer can be detected in solution, indicated by a doublet centered at δ = 356.0 and a triplet centered at δ = 148.5 ppm with a $^1J_{PP}$ coupling constant of 360 Hz. In contrast, for **10**, the bent isomer is also energetically favored by 22.1 kJ/mol, but both can be detected in solution in a solvent- and temperature-dependent equilibrium.[20] Due to the isolobal analogy between {Cp^{R}Ni} and P, complex **18** is isolobal to the *cyclo*-P$_4$ complex [Cp‴Co(η^4-P$_4$)].[30] Contrary to expectations, the reaction of **18** with Ag[FAl] does not lead to an oxidized complex but instead to the coordination compound [(Cp‴Co)(Cp″Ni)(μ$_4$,η^3:η^2:η^1:η^1-P$_3$){Ag(CH$_2$Cl$_2$)}]$_2$[FAl]$_2$ (**19**) (Scheme 4). Crystals suitable for X-ray single crystal structure analysis could be obtained from a concentrated solution in CH$_2$Cl$_2$ layered with hexane at room temperature. The structure in the solid state (Figure 5) shows a dimeric structural motif with a central six-membered ring consisting of two Ag atoms saturated each by a CH$_2$Cl$_2$ molecule and two P atoms of each molecule **18**. Initially targeting to obtain the analog copper coordination compound, we reacted **18** with [Cu(MeCN)$_{3.5}$][FAl]

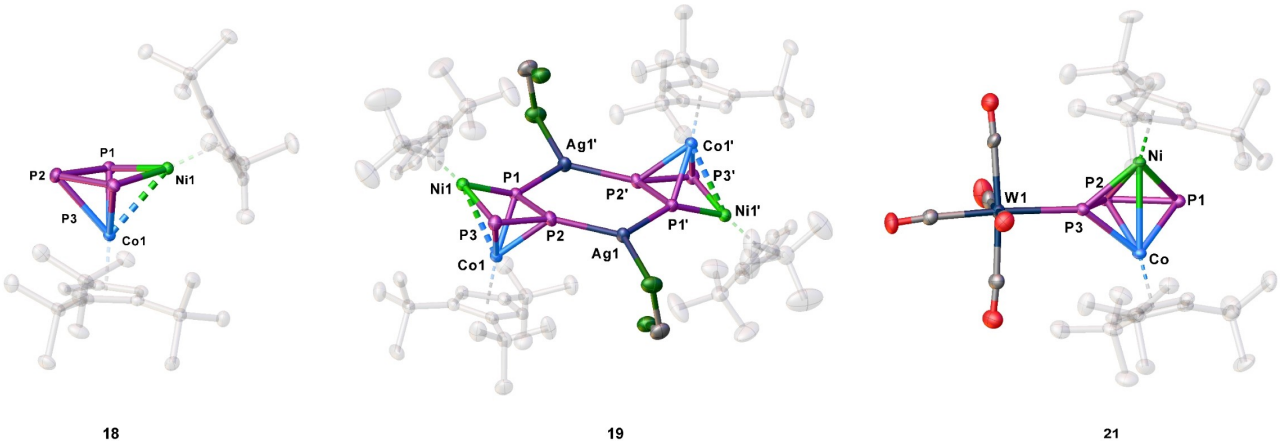

Figure 5. Molecular structures of **18**, **19** and **21** in the solid state. Thermal ellipsoids are drawn with 50% probability level. Hydrogen atoms, solvent molecules and anions, respectively, are omitted for clarity

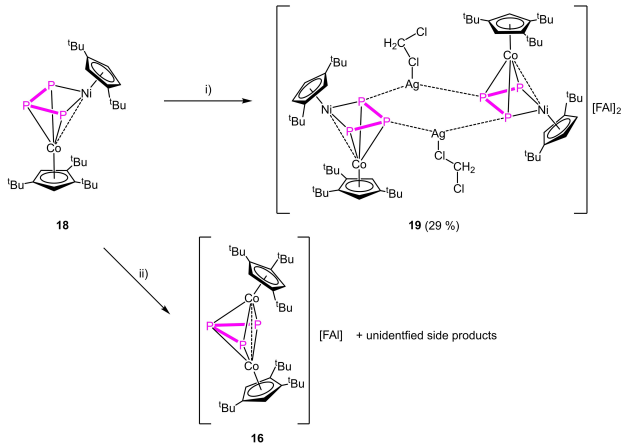

Scheme 4. Reaction of **18** with: i) Ag[FAl] and ii) $[Cu(MeCN)_{3,5}][FAl]$ in CH_2Cl_2 at room temperature.

(Scheme 4). Interestingly, a short time after the addition of the copper salt to **18**, a metal mirror was observed on the glass wall and, after workup, single crystals of **16** could be obtained, revealing clearly the transfer of $\{Cp^RM\}$ fragments during the oxidation process. It was not possible to identify further Cp′′Ni-containing products. The question arises as to whether the transfer of the metal fragments can be hindered. One possibility would be to coordinate an innocent organometallic fragment to the P_n ligand prior to oxidation. For this reason, we used the $\{W(CO)_5\}$-stabilized complex $[(Cp'''Co)(Cp'''Ni)(\mu_3,\eta^3{:}\eta^2{:}\eta^1\text{-}P_3)\{W(CO)_5\}]$ (**20**)[20] and reacted it with Ag[FAl]. Directly after addition of the silver salt, a metal mirror was observed and a ^{1}H NMR spectrum in CD_2Cl_2 was recorded showing the formation of new paramagnetic species. After stirring for one day, another NMR spectrum was recorded showing that the paramagnetic species was still present, not having disappeared as observed for the oxidation of **10** and **11**, respectively. After workup and crystallization, single crystals of $[(Cp'''Co)(Cp'''Ni)(\mu_3,\eta^3{:}\eta^3{:}\eta^1\text{-}P_3)\{W(CO)_5\}][FAl]$ (**21**) (Scheme 5)were obtained. The structure in the solid state reveals a strongly bent triple-decker geometry where one of the outer P atoms is coordinated to a $\{W(CO)_5\}$ fragment. Since both metal fragments contain the same Cp′′′ ligand, a mixed occupancy could not be dismissed. The paramagnetism of **21** is in agreement with two different metal atoms. The X-band EPR spectra of the obtained crystals shows a

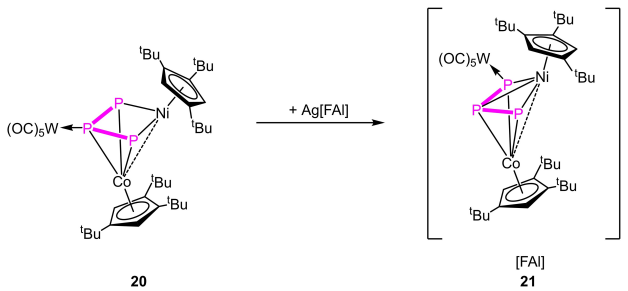

Scheme 5. Oxidation of **20** with Ag[FAl] in CH_2Cl_2.

rhombic resonance at room temperature and 77 K, the latter being simulated (cf. Figure S12, $g_1 = 2.060$, $g_2 = 2.007$, $g_3 = 1.984$, $g_{iso} = 2.017$). The ^{1}H NMR spectrum in CD_2Cl_2 reveals three very broad signals centered at $\delta = 5.73$, 2.01 and 1.74 ppm.

As already mentioned, the cyclic voltammograms of both **10** and **11** reveal possible reduction processes. The reduction of **10** and **11** yields $[K(2,2,2\text{-crypt})][(Cp'''Co)(Cp'''Ni)(\mu_3,\eta^3{:}\eta^3\text{-}E_3)]$ (E = P (**22**), As (**23**), Scheme 3) in crystalline yields of 76 % and 73 %, respectively. Crystals suitable for X-ray single crystal structure analysis could be obtained from a concentrated solution in thf layered with hexane at room temperature. The molecular structure in the solid state (Figure 4) shows a triple-decker complex with both Cp′′′ ligands being almost parallel to each other (Cp′′′NiCoCp′′′ angle of 174.1° (**22**) and 174.9° (**23**)). The E_3 middle deck shows two shorter E–E bonds (P1-P2 2.1792(10) Å, P2-P3 2.172(1) Å, As1-As2 2.362(12) Å, As2-As3 2.4327(7) Å) and two longer E···E contacts (P1-P3 2.5537(11) Å, As1-As3 2.7799)10) Å). The short distances are in the range between single and double bonds, indicated by the calculated WBIs of 1.04/1.08 for **22** and 0.99/1.02 for **23**. The long distances are too long to be considered as bonds, but an interaction should be present, indicated by the WBIs of 0.45 (**22**) and 0.68 (**23**). Compounds **22** and **23** are both paramagnetic, which agrees with the addition of one electron by the reduction process and no rearrangement as in the oxidations mentioned above took place. The related ^{1}H NMR spectra in thf-d_8 reveal several broad and partially strongly shifted signals. The magnetic moments in solution were determined by the Evans method to be 1.92 (**22**) and 1.22 (**23**) μ_B corresponding to roughly one unpaired electron each. At room temperature, the X-band EPR spectra of solid **22** show only a very weak resonance and, at 77 K, a strong resonance with a rhombic character. In contrast, the spectra of a thf solution of **22** show at room temperature a resonance with a poorly resolved hyperfine coupling and, at 77 K, a strong resonance with a hyperfine coupling to cobalt and phosphorus (Figure 6). The latter was simulated ($g_1 = 2.143$, $g_2 = 2.120$, $g_3 = 1.980$, $g_{iso} = 2.081$, $A_1^{Co} = 149$ MHz, $A_2^{Co} = 50$ MHz, $A_3^{Co} = 43$ MHz, $A_1^{P} = 14$ MHz, $A_2^{P} = 36$ MHz, $A_3^{P} = 42$ MHz). Compound **23** is EPR-silent at room temperature. The X-band EPR spectrum in a frozen thf solution at 77 K shows a rhombic resonance with a poorly resolved hyperfine coupling to cobalt, while the spectrum of solid **23** shows a rhombic signal without a resolved coupling (Figure 6, $g_1 = 2.214$, $g_2 = 2.142$, $g_3 = 2.039$, $g_{iso} = 2.146$). DFT calculations (BP86/def2-TZVP level of theory) reveal that the spin density is mainly located on the Co and only slightly on the Ni atom. In the case of **22**, also an additional small contribution of the P_3 ligand is observed. The reduction of **10** and **11** to **22** and **23** is fully reversible upon addition of $AgBF_4$.

Conclusion

It was shown that heterobimetallic triple-decker complexes possessing a polypnictogen ligand as middle deck show a versatile redox chemistry. They respond to the redox reaction either with slight changes in the geometry, in the fragmenta-

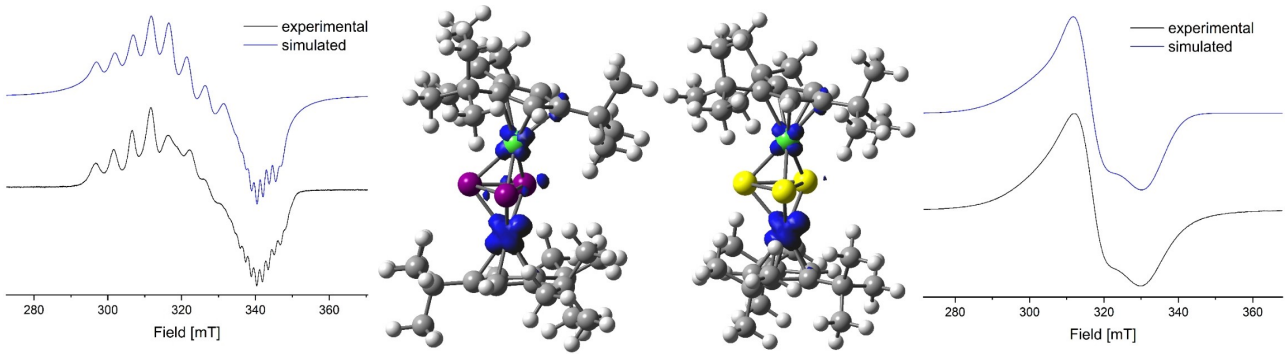

Figure 6. Experimental (black) and simulated (blue) X-band EPR spectra of **22** (left) in frozen thf solution and **23** (right) in the solid state and the iso-surfaces of the calculated spin density (BP86/def2-TZVP level of theory) in **22** (left middle) and **23** (right middle).

tion of the E_n ligand or in the exchange of {Cp‴M} fragments under formation of homometallic complexes. The iron and cobalt triple-decker complexes [(Cp*Fe)(Cp‴Co)(μ,η^5:η^4-E_5)] (E = P (**1**), As (**2**)) can be oxidized twice and reduced once, although the reduction of **2** is accompanied by a fragmentation of the As_5 ligand into As_6 and As_3-containing species. The folding of the *cyclo*-E_5 ligand is strongly dependent on the oxidation state. While oxidation leads to a successive planarization of the middle decks, reduction increases the fold angle and the coordination of the bent E atom changes from iron to cobalt. While in this case the outcome of the reduction is dependent on the pnictogen atom, this does not apply for the cobalt nickel triple-decker complexes [(Cp‴Co)(Cp‴Ni)(μ,η^3:η^3-E_3)] (E = P (**10**), As (**11**). Both can be reduced to **22** and **21**, while the oxidation to the heterometallic cations **12** and **13** does not display the end of the reaction, but a strong tendency to rearrange to the homo-metallic cobalt complexes **16** and **17** and the nickel complexes **14** and **15** is observed. The transfer of {Cp‴M} fragments was further investigated by EPR and NMR spectroscopy. Directly after the reaction, paramagnetic species (**12** and **13**) are present, which completely convert within one day into the homometallic diamagnetic compounds (**14**-**17**). Since both metal fragments contain the same Cp‴ ligand, the analog starting material with two different Cp ligands was prepared and analog reactions performed, revealing the same transfer of {Cp‴M} fragments upon oxidation. This transfer can be remediated when an innocent ligand ({$W(CO)_5$} is coordinated prior to the oxidation. The reversibility of the mentioned redox processes is very good for the mixed iron and cobalt complexes **1** and **2** (except reduction of **2**) and comparable with the homometallic triple-decker complexes mentioned in the introduction. For the mixed cobalt and nickel complexes **10** and **11**, only the reduction is reversible, while the oxidation is accompanied by an exchange of the {Cp‴M} fragments to form homometallic species.

Experimental Section

Synthetic procedures: All manipulations were performed under an atmosphere of dry argon using standard glove-box and Schlenk techniques. All solvents were degassed and purified by standard procedures. The compounds $[Cp‴Ni(CO)]_2$,[31] [(Cp*Fe)(Cp‴Co)(-μ,η^5:η^4-E_5)] (E = P (**1**), As (**2**)),[20,21] $[KC_8]$,[32] Ag[FAl],[33] $[Cu(MeCN)_{3.5}][FAl]$,[34] [(Cp‴Co)(Cp‴Ni)(μ,η^3:η^3-P_3)] (**10**),[20] [(Cp‴Co)(Cp‴Ni)(μ,η^3:η^2:η^1-P_3){$W(CO)_5$}] (**20**),[20] [Cp″Ni(η^3-P_3)],[35] $[(Cp‴Co)_2(η^4:η^4\text{-}C_7H_8)]$.[36] 18-c-6 and 2,2,2-cryptand were purchased commercially. The NMR spectra were recorded with a Bruker Avance 400 spectrometer (^{1}H: 400.13 MHz, ^{31}P: 161.976 MHz). The chemical shifts are given in ppm referenced to external $SiMe_4$ (^{1}H) and H_3PO_4 (^{31}P). Elemental analyses were determined with an Elementar Vario EL III apparatus. The X-Band EPR measurements were carried out with a MiniScope MS400 device with a frequency of 9.44 GHz and a rectangular resonator TE102 of the company Magnettech GmbH. The LIFDI-MS spectra were recorded with a Finnigan MAT 95 mass spectrometer. The ESI-MS spectra were acquired on a ThermoQuest Finnigan MAT TSQ 7000 mass spectrometer.

Synthesis of [Cp‴Ni(η^3-As_3)]: A freshly prepared solution of yellow arsenic in boiling xylene (starting from 5 g grey arsenic) was reacted with $[(Cp‴Ni(CO)]_2$ (800 mg, 6.248 mmol) under reflux for three hours. Five batches were combined and worked up together. The solvent was removed *in vacuo*, the residue dissolved in CH_2Cl_2 and SiO_2 was added. The preabsorbed reaction mixture was purified by column chromatography (SiO_2, hexane, 15×4.5 cm). Using hexane, an intense red fraction was eluted. The solvent was removed in vacuo and the oily residue dissolved in CH_2Cl_2 and precipitated with MeCN yielding a red powder. Yield: 3.70 g (57%). ^{1}H NMR (CD_2Cl_2, 25 °C): δ [ppm] = 5.45 (s, 2H, $C_5H_2{}^tBu_3$), 1.28 (s, 18H, $C_5H_2{}^tBu_3$), 1.10 (s, 9H, $C_5H_2{}^tBu_3$). FD-MS (toluene): *m/z* = 1250.0 (53%, $[(Cp‴Ni)_3As_5]$),), 882.0 (100%, $[(Cp‴Ni)_2As_4]$),), 807.0 (63%, $[(Cp‴Ni)_2As_3]$), 515.9(41%, $[M]^+$). EA $C_{17}H_{29}NiAs_3$: calc [%]: C 39.50; H 5.66; found [%]: C 39.15; H 5.27.

Synthesis of [(Cp*Fe)(Cp‴Co)(μ,η^5:η^5-P_5)][FAl] (3): A solution of Ag[FAl] (233.8 mg, 0.157 mmol, 1 eq) in CH_2Cl_2 was added to a stirred solution of **1** (100 mg, 0.157 mmol, 1 eq) in CH_2Cl_2 at room temperature, while the color changed from dark red to brown-green and a dark precipitate (Ag^0) was obtained. After stirring for 1 h, the reaction mixture was filtered over diatomaceous earth. The solvent of the green solution was reduced, layered with hexane and stored at −30 °C. After a few days, **3** could be obtained as green plates. The supernatant was decanted off, washed with hexane and dried *in vacuo*. Yield: 174 mg (55%). ^{1}H NMR (CD_2Cl_2, 25 °C): δ [ppm] = 5.66 (br, $\omega_{1/2}$ = 13 Hz, 15H, C_5Me_5), 3.76 (br, $\omega_{1/2}$ = 45 Hz 9H, $C_5H_2{}^tBu_3$), 3.29 (br, $\omega_{1/2}$ = 42 Hz 18H, $C_5H_2{}^tBu_3$), −65.22 (br, $\omega_{1/2}$ = 622 Hz, 2H, $C_5H_2{}^tBu_3$). ^{19}F{^{1}H} NMR (CD_2Cl_2, 25 °C): δ [ppm] = −112.6 (d, $J_{F\text{-}F}$ = 285 Hz, 6F), −117.1 (d, $J_{F\text{-}F}$ = 279 Hz, 6F), −121.8 (d, $J_{F\text{-}F}$ = 279 Hz,

3F), −127.9 (s, 6F), −130.6 (d, J_{F-F} = 274 Hz, 6F), −137.2 (d, J_{F-F} = 276 Hz, 6F), −141.2 (d, J_{F-F} = 274 Hz, 3F), −154.3 (t, J_{F-F} = 22 Hz, 6F), −165.0 (t, J_{F-F} = 18 Hz, 6F), −172.0 (s, AlF, 1F). $^{31}P\{^1H\}$ NMR (CD_2Cl_2, 25 °C): δ [ppm] = 275.1 (br, $\omega_{1/2}$ = 2600 Hz, P_5). ^{31}P NMR (CD_2Cl_2, 25 °C): δ [ppm] = 275.1 (br, $\omega_{1/2}$ = 2600 Hz, P_5). Evans-NMR (CD_2Cl_2, 25 °C): μ_{eff} = 2.04 μ_B corresponding to 1.27 unpaired electrons. ESI-MS (CH_2Cl_2): *m/z* = 638.1 (100 %, $[M]^+$), 607.1 (1 %, $[M-P]^+$). EA $C_{63}H_{44}O_3AlF_{46}P_5FeCo$: calc [%]: C 37.47; H 2.20; found [%]: C 37.46; H 2.31. X-band EPR (77 K, frozen CH_2Cl_2 solution) g_1 = 2.155, g_2 = 2.035, g_3 = 1.948, A_1^{Co} = 290.125, A_2^{Co} = 55.125, A_3^{Co} = 120.125 MHz, (77 K, solid) (overall shape similar to (77 K, liquid), but coupling not resolved).

Synthesis of [(Cp*Fe)(Cp‴Co)(μ,η⁵:η⁵-As₅)][FAl] (4): A solution of Ag[FAl] (173.5 mg, 0.1165 mmol, 1 eq) in CH_2Cl_2 was added to a stirred solution of **2** (100 mg, 0.1165 mmol, 1 eq) in CH_2Cl_2 at room temperature, while the color changed from dark green to brown-green and a dark precipitate (Ag^0) was obtained. After stirring for 1 h, the reaction mixture was filtered over diatomaceous earth. The solvent of the brown-green solution was reduced, layered with hexane and stored at −30 °C. After a few days, **4** could be obtained as brown plates. The supernatant was decanted off, washed with hexane and dried *in vacuo*. Yield: 165 mg (63 %). ^1H NMR (CD_2Cl_2, 25 °C): δ [ppm] = 3.84 (br, $\omega_{1/2}$ = 167 Hz, 9H, $C_5H_2{}^tBu_3$), 2.74 (br, $\omega_{1/2}$ = 119 Hz, 18H, $C_5H_2{}^tBu_3$), −1.09 (br, $\omega_{1/2}$ = 40 Hz, 15H, C_5Me_5). $^{19}F\{^1H\}$ NMR (CD_2Cl_2, 25 °C): δ [ppm] = −112.6 (d, J_{F-F} = 285 Hz, 6F), −117.1 (d, J_{F-F} = 279 Hz, 6F), −121.8 (d, J_{F-F} = 279 Hz, 3F), −127.9 (s, 6F), −130.6 (d, J_{F-F} = 274 Hz, 6F), −137.2 (d, J_{F-F} = 276 Hz, 6F), −141.2 (d, J_{F-F} = 274 Hz, 3F), −154.3 (t, J_{F-F} = 22 Hz, 6F), −165.0 (t, J_{F-F} = 18 Hz, 6F), −172.0 (s, AlF, 1F). Evans-NMR (CD_2Cl_2, 25 °C): μ_{eff} = 1.90 μ_B corresponding to 1.14 unpaired electrons. ESI-MS (CH_2Cl_2): *m/z* = 857.9 (100 %, $[M]^+$), 782.9 (67 %, $[M-As]^+$), 708.0 (13 %, $[M-2As]^+$). EA $C_{63}H_{44}O_3AlF_{46}As_5FeCo$: calc [%]: C 33.79; H 1.98; found [%]: C 34.06; H 2.01. X-band EPR (77 K, solid) g_1 = 2.235, g_2 = 1.952, g_3 = 1.896, (77 K, frozen CH_2Cl_2 solution) g_{iso} = 2.04, (r.t, CH_2Cl_2 solution) g_{iso} = 2.06, (r.t, solid) g_{iso} = 2.04.

Synthesis of [(Cp*Fe)(Cp‴Co)(μ,η⁵:η⁵-P₅)][FAl]₂ (5): A solution of Ag[FAl] (238 mg, 0.160 mmol, 2.05 eq) in *o*-$C_6H_4F_2$ was added to a stirred solution of **1** (50 mg, 0.078 mmol, 1 eq) in *o*-$C_6H_4F_2$ at room temperature, while the color changed from dark red to brown and a dark precipitate (Ag^0) was obtained. After stirring for 1 h, the reaction mixture was filtered over diatomaceous earth. The solvent of the brown solution was reduced, layered with toluene and stored at −30 °C. After a few days, **5** could be obtained as brown blocks. The supernatant was decanted off, washed with hexane and dried *in vacuo*. Yield: 131 mg (49 %). ^1H NMR (CD_2Cl_2, 25 °C): δ [ppm] = 4.69 (s, 2H, $C_5H_2{}^tBu_3$), 1.49 (s, 18H, $C_5H_2{}^tBu_3$), 1.39 (s, 9H, $C_5H_2{}^tBu_3$), 1.21 (s, 15H, C_5Me_5). $^{19}F\{^1H\}$ NMR (CD_2Cl_2, 25 °C): δ [ppm] = −112.6 (d, J_{F-F} = 285 Hz, 6F), −117.1 (d, J_{F-F} = 279 Hz, 6F), −121.8 (d, J_{F-F} = 279 Hz, 3F), −127.9 (s, 6F), −130.6 (d, J_{F-F} = 274 Hz, 6F), −137.2 (d, J_{F-F} = 276 Hz, 6F), −141.2 (d, J_{F-F} = 274 Hz, 3F), −154.3 (t, J_{F-F} = 22 Hz, 6F), −165.0 (t, J_{F-F} = 18 Hz, 6F), −172.0 (s, AlF, 1F). $^{31}P\{^1H\}$ NMR (CD_2Cl_2, 25 °C): δ [ppm] = 54.7 (s, P_5). ^{31}P NMR (CD_2Cl_2, 25 °C): δ [ppm] = 54.7 (s, P_5). ESI-MS (CH_2Cl_2): *m/z* = 638.1 (100 %, $[M]^+$). ESI-MS (o-$C_6H_4F_2$): *m/z* = 638.1 (100 %, $[M]^+$), 319.0 (7 %, $[M]^{2+}$). EA $C_{99}H_{44}O_6Al_2F_{92}P_5FeCo$ x $C_6H_4F_2$: calc [%]: C 35.88; H 1.37; found [%]: C 35.58; H 1.42.

Synthesis of [(Cp*Fe)(Cp‴Co)(μ,η⁵:η⁵-As₅)][FAl]₂ (6): A solution of Ag[FAl] (375 mg, 0.2518 mmol, 2 eq) in o-$C_6H_4F_2$ was added to a stirred solution of **2** (108 mg, 0.1259 mmol, 1 eq) in o-$C_6H_4F_2$ at room temperature, while the color changed from dark green to brown and a dark precipitate (Ag^0) was obtained. After stirring for 4 h, the reaction mixture was filtered over diatomaceous earth. The solvent of the brown solution was reduced, layered with toluene and stored at −30 °C. After a few days, **6** could be obtained as brown blocks. The supernatant was decanted off, washed with hexane and dried *in vacuo*. Yield: 344 mg (75 %). ^1H NMR (o-$C_6H_4F_2$ + C_6D_6 capillary, 25 °C): δ [ppm] = 4.20 (s, 2H, $C_5H_2{}^tBu_3$), 1.25 (s, 18H, $C_5H_2{}^tBu_3$), 1.18 (s, 9H, $C_5H_2{}^tBu_3$), 0.86 (s, 15H, C_5Me_5). $^{19}F\{^1H\}$ NMR (o-$C_6H_4F_2$ + C_6D_6 capillary, 25 °C): δ [ppm] = −112.6 (d, J_{F-F} = 285 Hz, 6F), −117.1 (d, J_{F-F} = 279 Hz, 6F), −121.8 (d, J_{F-F} = 279 Hz, 3F), −127.9 (s, 6F), −130.6 (d, J_{F-F} = 274 Hz, 6F), −137.2 (d, J_{F-F} = 276 Hz, 6F), −141.2 (d, J_{F-F} = 274 Hz, 3F), −154.3 (t, J_{F-F} = 22 Hz, 6F), −165.0 (t, J_{F-F} = 18 Hz, 6F), −172.0 (s, AlF, 1F). ESI-MS (o-$C_6H_4F_2$): *m/z* = 857.8 (56 %, $[M]^+$), 428.9 (100 %, $[M]^{2+}$). EA $C_{99}H_{44}O_6Al_2F_{92}P_5FeCo$: calc [%]: C 32.84; H 1.22; found [%]: C 32.55; H 1.46.

Synthesis of [K(2,2,2-crypt)][(Cp*Fe)(Cp‴Co)(μ,η⁴:η³-P₅)] (7): A suspension of KC_8 (25 mg, 0.188, 1. 2 eq) in dme was added to a stirred solution of **1** (100 mg, 0.1567 mmol, 1 eq) and 2,2,2-crypt (59 mg, 0.1567 mmol, 1 eq) in dme, while the color changed from dark red to brown green. After stirring for 3 h it was filtered over diatomaceous earth. The solvent was reduced and layered with hexane at room temperature. **7** could be obtained as dark green blocks. The supernatant was decanted off and the crystals dried in vacuo. Yield: 88 mg (44 %) ^1H NMR (thf-d_8, 25 °C): δ [ppm] = 6.24 (br, 9H, $C_5H_2{}^tBu_3$), 4.15 (br, 15H, C_5Me_5), 3.70 (br, 12H, crypt), 3.66 (br, 12H, cypt), 3.44 (br, 18H, $C_5H_2{}^tBu_3$), 2.66 (br, 12 H, crypt). EA $C_{45}H_{80}O_6N_2P_5FeCoK$: calc [%]: C 51.29; H 7.65; N 2.66; found [%]: C 51.21; H 7.35; N 2.57. Evans-NMR (thf-d_8, 25 °C): μ_{eff} = 2.01 μ_B corresponding to 1.24 unpaired electrons. X-band EPR (77 K, solid) g_{iso} = 2.047, (77 K, frozen dme solution) g_{iso} = 2.041, (r.t, dme solution) g_{iso} = 2.078, (r.t, solid) g_{iso} = 2.060.

Reaction of [(Cp*Fe)(Cp‴Co)(μ,η⁵:η⁴-As₅)] (2) with KC_8: Compound **2** (100 mg, 0.1166 mmol, 1 eq), KC_8 (19 mg, 0.1399, 1.2 eq) and 2,2,2-crypt (43.9 mg, 0.1166 mmol, 1 eq) were weighed in together and dimethoxyethane was added, while the color changed from dark green to brown. After stirring for 5 minutes, it was filtered over diatomaceous earth and the solvent was reduced. An excess of hexane was used for precipitation. The microcrystalline solid was washed with hexane (slight brown to green color) and dried *in vacuo*. The ^1H NMR spectrum in thf-d_8 reveals the formation of **9** beside the paramagnetic compound [K(2,2,2-crypt)][(Cp*Fe)(Cp‴-Co)(μ,η⁴:η³-As₅)] (**8**) (cf. Figure S24). X-Band EPR measurement of the obtained solid reveals a strong isotropic resonance. Compound **8**: X-band EPR (77 K, solid) g_{iso} = 2.123, (r.t, solid) g_{iso} = 2.109.

Synthesis of [K(2,2,2-crypt)][(Cp*Fe)(Cp‴Co)(μ,η⁴:η⁴-As₆)] (9): Compound **2** (500 mg, 0.5827 mmol, 1 eq), KC_8 (88 mg, 0.651, 1.12 eq) and 2,2,2-crypt (219.5 mg, 0.5827 mmol, 1 eq) were weighed in together and dimethoxyethane was added. After stirring overnight (color change from green to brown), it was filtered over diatomaceous earth. The solvent was reduced and layered with hexane at room temperature. After a few days, an oily solid was observed at the Schlenk wall. Leaving it for a few weeks, crystalline solid (needles) of **9** were obtained. The supernatant was decanted off, washed with hexane and the crystals dried *in vacuo*. The ^1H NMR spectrum of the brown-green mother liquor reveals [(Cp*Fe)(Cp‴-Co)(μ,η³:η³-As₃)][21] as a major compound. Yield: 481 mg (92 %). ^1H NMR (thf-d_8, 25 °C): δ [ppm] = 4.14 (s, 2H, $C_5H_2{}^tBu_3$), 3.61 (s, 12H, $C_{18}H_{36}N_2O_6$), 3.57 (overlapped with solvent signal, $C_{18}H_{36}N_2O_6$), 2.56 (t, $^3J_{HH}$ = 4.4 Hz, 12H, $C_{18}H_{36}N_2O_6$), 1.61 (s, 15H, C_5Me_5), 1.53 (s, 18H, $C_5H_2{}^tBu_3$), 1. 35 (s, 9H, $C_5H_2{}^tBu_3$). ESI-MS (dme): *m/z* = 932.9 (100 %, $[M]^-$). EA $C_{45}H_{80}O_6N_2As_6FeCoK$: calc [%]: C 40.08; H 5.98; N 2.08; found [%]: C 40.60; H 6.12; N 1.94.

Synthesis of [(Cp‴Co)(Cp‴Ni)(μ,η³:η³-As₃)] (11): A solution of $[(Cp'''Co)_2(\mu,\eta^4{:}\eta^4\text{-}C_7H_8)]$ (985 mg, 1.455 mmol, 1 eq) in hexane was added to a stirred solution of $[Cp'''Ni(\eta^3\text{-}As_3)]$ (1.50 mg, 2.91 mmol, 2 eq) in hexane at room temperature, while the color changed to green. After stirring for one hour, the solvent was removed *in vacuo*. The residue was dissolved in CH_2Cl_2 and layered with MeCN

and stored at room temperature. After a few days, **11** can be obtained as green needles. The supernatant was decanted off and the remaining crystals dried *in vacuo*. Yield: 2.05 g (85%). **^{1}H NMR** (C_6D_6, 25 °C): δ [ppm] = 5.14 (s, *2H*, $C_5H_2{}^t$Bu$_3$), 4.90 (s, *2H*, $C_5H_2{}^t$Bu$_3$), 1.43 (s, 18H, $C_5H_2{}^tBu_3$), 1.34 (s, 18H, $C_5H_2{}^tBu_3$), 1.06 (s, 9H, $C_5H_2{}^tBu_3$), 0.96 (s, 9H, $C_5H_2{}^tBu_3$). **LIFDI-MS** (toluene): *m/z* = 808.0 (100%, $[M]^+$). **EA** $C_{34}H_{58}CoNiAs_3$: calc [%]: C 50.46; H 7.22; found [%]: C 50.07; H 6.84.

Reaction of [(Cp‴Co)(Cp‴Ni)(μ,η^3:η^3-P$_3$)] (10) with Ag[FAl]: A solution of Ag[FAl] (220 mg, 0.148 mmol, 1 eq) in CH_2Cl_2 was added to a stirred solution of **10** (100 mg, 0.148 mmol, 1 eq) in CH_2Cl_2 at −80 °C. The reaction mixture was warmed to room temperature, while a color change from brown to red-brown and a dark precipitate (Ag^0) was observed. The desired [(Cp‴Co)(Cp‴Ni)(-μ,η^3:η^3-P$_3$)][FAl] (**12**) was precipitated by addition of hexane, the solvent was decanted off and the residue dried *in vacuo*. The obtained solid was investigated by NMR and EPR spectroscopy, revealing the paramagnetic character of **12**. ^{1}H NMR (CD_2Cl_2, 25 °C): δ [ppm] = 3.65 (br, $\omega_{1/2}$ = 127 Hz, 27H, $C_5H_2{}^tBu_3$), 2.96 (br, $\omega_{1/2}$ = 53 Hz, 18H, $C_5H_2{}^tBu_3$), 2.49 (br, $\omega_{1/2}$ = 48 Hz, 9H, $C_5H_2{}^tBu_3$). X-band EPR (r.t, solution) g_{iso} = 2.023, g_1 = 2.023, g_2 = 2.031, g_3 = 2.014, A_1^{Co} = 59.56, A_2^{Co} = 63.97, A_3^{Co} = 62.83 MHz; (77 K, frozen CH_2Cl_2 solution) g_{iso} = 2.025.

Oxidation of [(Cp‴Co)(Cp‴Ni)(μ,η^3:η^3-As$_3$)] (11): A solution of Ag[FAl] (92 mg, 0.062 mmol, 1 eq) in CH_2Cl_2 was added to a stirred solution of **11** (50 mg, 0.062 mmol, 1 eq) in CH_2Cl_2 at −80 °C, while the color changed from green to red-brown. The reaction mixture was warmed to room temperature and a dark precipitate (Ag^0) was observed. The desired [(Cp‴Co)(Cp‴Ni)(μ,η^3:η^3-As$_3$)][FAl] (**13**) was precipitated by addition of hexane, the solvent was decanted off and the residue dried *in vacuo*. The obtained solid was investigated by ^{1}H NMR and EPR spectroscopy, revealing the paramagnetic character of **13**. The residual solid was again dissolved in CH_2Cl_2 and stirred for five days. The solvent was removed in vacuo and an ^{1}H NMR spectrum in CD_2Cl_2 was recorded, revealing the formation of the two diamagnetic species [(Cp‴Co)$_2$(μ,η^3:η^3-As$_3$)][FAl] (**17**) and [(Cp‴Ni)$_2$(μ,η^3:η^3-As$_3$)][FAl] (**15**). Very few single crystals of **17** suitable for X-ray diffractions were obtained by layering a concentrated solution of the reaction mixture in *o*-$C_6H_4F_2$ with pentane at −30 °C. Analytically pure **15** can be obtained by the oxidation of [Cp‴Ni(η^3-As$_3$)] with diacetyl-ferrocenium (vide infra). Analytical data of **13**: ^{1}H NMR (CD_2Cl_2, 25 °C): δ [ppm] = 3.04 (br, 18H, $C_5H_2{}^tBu_3$), 2.99 (br,9H, $C_5H_2{}^tBu_3$), 2.76 (br, 18H, $C_5H_2{}^tBu_3$), 2.25 (br, 18H, $C_5H_2{}^tBu_3$), −23.51 (br, 2H, $C_5H_2{}^t$Bu$_3$). X-band EPR (77 K, solid) g_1 = 2.155, g_2 = 2.071, g_3 = 2.016, (77 K, frozen CH_2Cl_2 solution) g_{iso} = 2.070.

Oxidation of [Cp‴Ni(η^3-As$_3$)]: Addition of a blueish green solution of [Fc^{Diac}][FAl] (83 mg, 0.05 mmol, 0.5 eq.) in CH_2Cl_2 to a dark red solution of Cp‴Ni(η^3-As$_3$) (52 mg, 0.1 mmol, 1 eq.) in CH_2Cl_2 at −80 °C afforded a rapid color change to dark brown. The reaction mixture was left to warm to room temperature and stirred for another 2 h. Afterwards pentane was added to precipitate **15** as a brown powder. The supernatant was decanted off, the solid washed two times with toluene and another two times with pentane. The residue was dissolved in CH_2Cl_2 and layered with pentane. After a few days, **15** could be obtained as brown blocks. The supernatant was decanted off and the crystals washed with hexane and dried *in vacuo*. Yield: 55 mg (50%). ^{1}H NMR (CD_2Cl_2, 25 °C): δ [ppm] = 5.09 (s, *2H*, $C_5H_2{}^t$Bu$_3$), 1.35 (s, 18H, $C_5H_2{}^tBu_3$), 0.96 (s, 9H, $C_5H_2{}^tBu_3$). ESI-MS (CH_2Cl_2): *m/z* = 841.1 (0.1%, $[M+H_2O+O]$), 807.1 (0.6%, $[M]^+$), 373.2 (24%, [Cp‴Ni(MeCN)$_2$]), 332.2 (100%, [Cp‴NiMeCN]). EA $C_{70}H_{58}O_3Ni_2As_3AlF_{46}$: calc [%]: C 38.39; H 2.67; found [%]: C 38.61; H 2.70.

Synthesis of [(Cp‴Co)$_2$(μ,η^3:η^3-P$_3$)][FAl] (16): A solution of Ag[FAl] (220 mg, 0.148 mmol, 1 eq) in CH_2Cl_2 was added to a stirred solution of **10** (100 mg, 0.148 mmol, 1 eq) in CH_2Cl_2 at room temperature, while the color changed from brown to red-brown and a dark precipitate (Ag^0) was obtained. The reaction was completed by stirring for 20 h (dark red color, shorter reaction times do not lead to a full conversion). The reaction mixture was filtered over diatomaceous earth. The ^{1}H and ^{31}P{^{1}H} NMR spectra in CD_2Cl_2 reveals the formation of [(Cp‴Co)$_2$(μ,η^3:η^3-P$_3$)][FAl] (**16**) and [(Cp‴Ni)$_2$(μ,η^3:η^3-P$_3$)][FAl] (**14**).[28] The solvent of the red solution was reduced, layered with toluene and stored at −30 °C. After a few days, **16** can be obtained as red rods. The supernatant was decanted off, washed with hexane and dried *in vacuo*. Yield: 86 mg (65%). **^{1}H NMR** (CD_2Cl_2, 25 °C): δ [ppm] = 4.89 (s, *4H*, $C_5H_2{}^t$Bu$_3$), 1.41 (s, 36H, $C_5H_2{}^tBu_3$), 1.23 (s, 18H, $C_5H_2{}^tBu_3$). **^{31}P{^{1}H} NMR** (CD_2Cl_2, 25 °C): δ [ppm] = 789.0 (d, $^1J_{PP}$ = 361 Hz, 2P, P_3), −218.0 (t, $^1J_{PP}$ = 361 Hz, 1P, P_3). **^{31}P NMR** (CD_2Cl_2, 25 °C): δ [ppm] = 789.0 (d, $^1J_{PP}$ = 361 Hz, 2P, P_3), −218.0 (t, $^1J_{PP}$ = 361 Hz, 1P, P_3). **^{19}F{^{1}H} NMR** (CD_2Cl_2, 25 °C): δ [ppm] = -112.6 (d, $J_{F\text{-}F}$ = 285 Hz, 6F), −117.1 (d, $J_{F\text{-}F}$ = 279 Hz, 6F), −121.8 (d, $J_{F\text{-}F}$ = 279 Hz, 3F), −127.9 (s, 6F), −130.6 (d, $J_{F\text{-}F}$ = 274 Hz, 6F), −137.2 (d, $J_{F\text{-}F}$ = 276 Hz, 6F), −141.2 (d, $J_{F\text{-}F}$ = 274 Hz, 3F), −154.3 (t, $J_{F\text{-}F}$ = 22 Hz, 6F), −165.0 (t, $J_{F\text{-}F}$ = 18 Hz, 6F), −172.0 (s, AlF, 1F). **ESI-MS** (CH_2Cl_2): *m/z* = 677.2 (100%, $[M]^+$). **EA** $C_{70}H_{58}O_3AlF_{46}Co_2P_3$: calc [%]: C 40.83; H 2.84; found [%]: C 40.91; H 3.12.

Synthesis of [(Cp‴Co)$_2$(μ,η^3:η^3-As$_3$)][FAl] (17):A solution of Ag[FAl] (184 mg, 0.1235 mmol, 1 eq) in CH_2Cl_2 was added to a stirred solution of **11** (100 mg, 0.1235 mmol, 1 eq) in CH_2Cl_2, while the color changed immediately from dark green to brown. The reaction mixture was stirred overnight and filtered over diatomaceous earth. The solvent was reduced, layered with hexane and stored at −30 °C. After a few days, **17** could be obtained as brown blocks, with **15** remaining in the mother liquor. The mother liquor was decanted off, the obtained crystals washed with hexane and dried in vacuo. Yield: 45 mg (17%).Analytical data of **17**: ^{1}H NMR (CD_2Cl_2, 25 °C): δ [ppm] = 4.79 (s, *2H*, $C_5H_2{}^t$Bu$_3$), 1.35 (s, 18H, $C_5H_2{}^tBu_3$), 1.15 (s, 9H, $C_5H_2{}^tBu_3$). ^{19}F{^{1}H} NMR (CD_2Cl_2, 25 °C): δ [ppm] = −112.6 (d, $J_{F\text{-}F}$ = 285 Hz, 6F), −117.1 (d, $J_{F\text{-}F}$ = 279 Hz, 6F), −121.8 (d, $J_{F\text{-}F}$ = 279 Hz, 3F), −127.9 (s, 6F), −130.6 (d, $J_{F\text{-}F}$ = 274 Hz, 6F), −137.2 (d, $J_{F\text{-}F}$ = 276 Hz, 6F), −141.2 (d, $J_{F\text{-}F}$ = 274 Hz, 3F), −154.3 (t, $J_{F\text{-}F}$ = 22 Hz, 6F), −165.0 (t, $J_{F\text{-}F}$ = 18 Hz, 6F), -172.0 (s, AlF, 1F).ESI-MS (CH_2Cl_2): *m/z* = 809.09 (100%, $[M]^+$). EA $C_{70}H_{58}O_3AlF_{46}Co_2As_3x(C_6H_4F_2)_{0.5}$: calc [%]: C 39.01; H 2.69; found [%]: C 38.89; H 2.62.

Synthesis of [(Cp‴Co)(Cp″Ni)(μ,η^3:η^2-P$_3$)] (18): A solution of [(Cp‴Co)$_2$(μ,η^4:η^4-C_7H_8) (680 mg, 1.00 mmol, 1 eq) in toluene was added to a stirred solution of [Cp″Ni(η^3-P$_3$)] (658 mg, 2.00 mmol, 2 eq) in toluene at room temperature. After stirring for one hour, the solvent was removed *in vacuo*. The residue was dissolved in CH_2Cl_2 and layered with MeCN and stored at −30 °C. After a few days, **18** was obtained as brown needles. The supernatant was decanted off and the remaining crystals dried *in vacuo*. Yield: 730 mg (59%). ^{1}H NMR (C_6D_6, 25 °C): δ [ppm] = 4.96 (s, *1H*, $C_5H_3{}^t$Bu$_2$), 4.81 (s, *2H*, $C_5H_3{}^t$Bu$_2$), 4.78 (s, *2H*, $C_5H_2{}^t$Bu$_3$), 1.39 (s, 18H, $C_5H_2{}^tBu_3$), 1.26 (s, 9H, $C_5H_2{}^tBu_3$), 1.23 (s, 18H, $C_5H_3{}^tBu_2$). ^{31}P{^{1}H} NMR (C_6D_6, 25 °C): δ [ppm] = 375.0 (d, $^1J_{PP}$ = 360 Hz, 2P, P_3), 148.5 (t, $^1J_{PP}$ = 360 Hz, 1P, P_3). LIFDI-MS (toluene): *m/z* = 620.1 (100%, $[M]^+$). EA $C_{30}H_{50}CoNiP_3$: calc [%]: C 57.99; H 8.11; found [%]: C 57.63; H 7.97.

Synthesis of [(Cp‴Co)(Cp″Ni)(μ$_4$,η^3:η^2:η^1:η^1-P$_3$)Ag(CH$_2$Cl$_2$)]$_2$[FAl]$_2$ (19): A solution of Ag[FAl] (240 mg, 0.161 mmol, 1 eq) in CH_2Cl_2 was added to a stirred solution of **18** (100 mg, 0.161 mmol, 1 eq) in CH_2Cl_2, while the color changed to red-brown. After stirring for two hours, the volume of the solvent was reduced and layered with hexane. After storage at room temperature for a few days, **19** could be obtained as brown blocks. The supernatant was decanted off and the remaining crystals dried *in vacuo*. Yield: 120 mg (29%). ^{1}H NMR (CD_2Cl_2, 25 °C): δ [ppm] = 4.93 (br, *3H*, $C_5H_3{}^t$Bu$_2$), 4.17 (br, *2H*,

$C_5H_2{}^tBu_3$), 1.51 (s, 9H, $C_5H_2{}^tBu_3/C_5H_3{}^tBu_2$), 1.49 (s, 9H, $C_5H_2{}^tBu_3/C_5H_3{}^tBu_2$), 1.43 (s, 9H, $C_5H_2{}^tBu_3/C_5H_3{}^tBu_2$), 1.22 (s, 18H, $C_5H_2{}^tBu_3/C_5H_3{}^tBu_2$). $^{31}P\{^1H\}$ NMR (CD_2Cl_2, 25 °C): δ [ppm] = 334.2 (br), 321.9 (br), 125.9 (br), 110.8 (br). ESI-MS (CH_2Cl_2): *m/z* = 1477.5 (100 %, $[M+F]^+$). EA $C_{67}H_{52}O_3CoNiP_3AgAlCl_2F_{46}\times 1.4\ CH_2Cl_2$: calc [%]: C 35.42; H 2.39; found [%]: C 35.28; H 2.30.

Synthesis of [(Cp‴Co)(Cp‴Ni)(μ,η³:η³:η¹-P₃){W(CO)₅}][FAl] (21): A solution of Ag[FAl] (149 mg, 0.10 mmol, 1 eq) in CH_2Cl_2 was added to a stirred solution of **20** (100 mg, 0.10 mmol, 1 eq) in CH_2Cl_2 and stirred overnight, while the color changed from red to brown and a dark precipitate (Ag^0) was observed. The reaction mixture was filtered over diatomaceous earth. The solvent was removed *in vacuo*. The residue was washed with hexane (slightly brown), dissolved in CH_2Cl_2, layered with hexane and stored at room temperature. After a few days, few crystals of **21** could be obtained in form of brown blocks. ^1H NMR (CD_2Cl_2, 25 °C): δ [ppm] = 5.73 (very broad, $C_5H_2{}^tBu_3$), 2.01 (br, *36H*, $C_5H_2{}^tBu_3$), 1.74 (br, *18H*, $C_5H_2{}^tBu_3$). $^{19}F\{^1H\}$ NMR (CD_2Cl_2, 25 °C): δ [ppm] = −112.6 (d, $J_{F\text{-}F}$ = 285 Hz, 6F), −117.1 (d, $J_{F\text{-}F}$ = 279 Hz, 6F), −121.8 (d, $J_{F\text{-}F}$ = 279 Hz, 3F), −127.9 (s, 6F), −130.6 (d, $J_{F\text{-}F}$ = 274 Hz, 6F), −137.2 (d, $J_{F\text{-}F}$ = 276 Hz, 6F), −141.2 (d, $J_{F\text{-}F}$ = 274 Hz, 3F), −154.3 (t, $J_{F\text{-}F}$ = 22 Hz, 6F), −165.0 (t, $J_{F\text{-}F}$ = 18 Hz, 6F), -172.0 (s, AlF, 1F). X-band EPR (293 K, solid) rhombic spectrum similar to the spectrum at 77 K, no simulation performed; (77 K, solid) g_{iso} = 2.017, g_1 = 2.060, g_2 = 2.007, g_3 = 1.984.

Synthesis of [K(2,2,2-crpyt)][(Cp‴Co)(Cp‴Ni)(μ,η³:η³-P₃)] (22): A suspension of KC_8 (25 mg, 0.18 mmol, 1.22 eq) in dimethoxyethane was added to a stirred solution of **10** (100 mg, 0.1476 mmol, 1 eq) and 2,2,2-cryptand (56 mg, 0.1476 mmol, 1 eq) in dimethoxyethane at −50 °C, while the color changed from brown to dark brown. The reaction mixture was allowed to reach room temperature overnight. The reaction mixture was filtered over diatomaceous earth, the solvent removed *in vacuo* and washed with hexane. The residue was dissolved in thf, layered with hexane and stored at room temperature. After a few days, **20** could be obtained as brown plates. The supernatant was decanted off, washed with hexane and dried *in vacuo*. Yield: 123 mg (76 %). ^1H NMR (thf-d_8, 25 °C): δ [ppm] = 3.65 (s, $C_{18}H_{36}N_2O_6$), 3.61 (s, $C_{18}H_{36}N_2O_6$), 2.78 (br, $C_5H_2{}^tBu_3$),2.62 (s, $C_{18}H_{36}N_2O_6$), 2.33 (br, $C_5H_2{}^tBu_3$), 1.63 (br, $C_5H_2{}^tBu_3$). Evans-NMR (thf-d_8, 25 °C): μ_{eff} = 1.92 μ_B; corresponding to roughly one unpaired electron. ESI-MS (dme): *m/z* = 676.2 (39 %, $[M]^-$), 385.1 (100 %, [M–Cp‴Ni]$^-$). EA $C_{52}H_{94}O_6N_2KCoNiP_3$: calc [%]: C 57.14; H 8.67, N 2.56; found [%]: C 57.22; H 8.50, N 2.52. X-band EPR (293 K, solid) g_{iso} = 2.079, (77 K, solid) g_{iso} = 2.061, (293 K, solution) rhombic spectrum with fine couplings, badly resolved, no simulation performed, (77 K, liquid) g_{iso} = 2.081, g_1 = 2.143, g_2 = 2.120, g_3 = 1.980, A_1^{Co} = 148.53, A_2^{Co} = 50.32, A_3^{Co} = 42.72, A_1^{P} = 13.63, A_2^{P} = 35.94, A_3^{P} = 42.13 MHz).

Synthesis of [K(2,2,2-crypt)][(Cp‴Co)(Cp‴Ni)(μ,η³:η³-As₃)] (23): A suspension of KC_8 (25 mg, 0.1900 mmol, 1.5 eq) in dimethoxyethane was added to a stirred solution of **16** (100 mg, 0.1236 mmol, 1 eq) and 2,2,2-cryptand (47 mg, 0.1236 mmol, 1 eq) in dimethoxyethane at room temperature, while the color changed from green to red-brown. After one hour, the reaction mixture was filtered over diatomaceous earth, the solvent removed *in vacuo* and washed with hexane. The residue was dissolved in thf, layered with hexane and stored at room temperature. After a few days, **23** could be obtained as brown blocks. The supernatant was decanted off, washed with hexane and dried *in vacuo*. Yield: 110 mg (73 %). ^1H NMR (thf-d_8, 25 °C): δ [ppm] = 3.61 (s, $C_{18}H_{36}N_2O_6$), 3.57 (s, overlapped with solvent signal, $C_{18}H_{36}N_2O_6$), 3.16 (br, $C_5H_2{}^tBu_3$),2.59 (br, $C_{18}H_{36}N_2O_6 + C_5H_2{}^tBu_3$), 1.41 (br, $C_5H_2{}^tBu_3$). Evans-NMR (thf-d_8, 25 °C): μ_{eff} = 1.22 μ_B; corresponding to roughly one unpaired electron. ESI-MS (dme): no fragments can be assigned properly. EA $C_{52}H_{94}N_2O_6KCoNiAs_3$: calc [%]: C 50.99; H 7.74; N 2.29; found [%]: C 51.22; H 7.21, N 2.23. 76. X-band EPR (77 K, solid) g_{iso} = 2.141, g_1 = 2.214, g_2 = 2.142, g_3 = 2.039, (77 K, solution) rhombic spectrum with fine couplings, badly resolved, no simulation performed.

Crystallographic data: Deposition numbers 2064647 (**3**), 2064648 (**4**), 2064649 (**5**), 2064650 (**6**), 2064651 (**7**), 2064652 (9), 2064653 (11), 2064654 (**15**), 2064655 (**16**), 2064656 (**17**), 2064657 (**18**), 2064658 (**19**), 2064659 (**21**), 2064660 (**22**), 2064661 (**23**) and 2064662 ([Cp‴Ni(η_3-As$_3$)]) contain the supplementary crystallographic data for this paper. These data are provided free of charge by the joint Cambridge Crystallographic Data Centre and Fachinformationszentrum Karlsruhe Access Structures service.

Acknowledgements

This work was supported by the Deutsche Forschungsgemeinschaft within the project Sche 384/33-2 and 384/36-1. M. P. is grateful to the Fonds der Chemischen Industrie for a PhD fellowship and S. R. is grateful to the Studienstiftung des Deutschen Volkes for a PhD fellowship. Open access funding enabled and organized by Projekt DEAL.

Conflict of Interest

The authors declare no conflict of interest.

Keywords: arsenic · heterometallic complexes• phosphorus · redox chemistry · transfer reactions

[1] a) G. Gnutzmann, F. Wilhelm Dorn, W. Klemm, *Z. Anorg. Allg. Chem.* **1961**, *309*, 210–225; b) M. Delamar, *J. Electroanal. Chem. Interfacial Electrochem.* **1975**, *63*, 339–349; c) G. Brauer, E. Zintl, *Z. physik. Chem.* **1937**, *B37*, 323–352.
[2] a) T. Köchner, T. A. Engesser, H. Scherer, D. A. Plattner, A. Steffani, I. Krossing, *Angew. Chem. Int. Ed.* **2012**, *51*, 6529–6531; *Angew. Chem.* **2012**, *124*, 6635–6637; b) R. J. Gillespie, J. Passmore, P. K. Ummat, O. C. Vaidya, *Inorg. Chem.* **1971**, *10*, 1327–1332.
[3] a) A. Tzschach, V. Kiesel, *J. Prakt. Chem.* **1971**, *313*, 259–264; b) M. Baudler, C. Gruner, G. Fürstenberg, B. Kloth, F. Saykowski, U. Özer, *Z. Anorg. Allg. Chem.* **1978**, *446*, 169–176.
[4] D. Astruc, *Eur. J. Inorg. Chem.* **2017**, *2017*, 6–29.
[5] G. Gritzner, J. Kuta, *Pure Appl. Chem.* **1984**, *56*, 461–466.
[6] a) K. Arumugam, C. D. Varnado, S. Sproules, V. M. Lynch, C. W. Bielawski, *Chem. Eur. J.* **2013**, *19*, 10866–10875; b) A. M. Allgeier, C. A. Mirkin, *Angew. Chem. Int. Ed.* **1998**, *37*, 894–908; *Angew. Chem.* **1998**, *110*, 936–952.
[7] P. Neumann, H. Dib, A.-M. Caminade, E. Hey-Hawkins, *Angew. Chem. Int. Ed.* **2015**, *54*, 311–314; *Angew. Chem.* **2015**, *127*, 316–319.
[8] R. S. P. Turbervill, A. R. Jupp, P. S. B. McCullough, D. Ergöçmen, J. M. Goicoechea, *Organometallics* **2013**, *32*, 2234–2244.
[9] a) F. Nief, L. Ricard, *Organometallics* **2001**, *20*, 3884–3890; b) S. Du, Z. Chai, J. Hu, W.-X. Zhang, Z. Xi, *Chin. J. Org. Chem.* **2019**, *39*, 2338; c) S. Du, J. Yin, Y. Chi, L. Xu, W.-X. Zhang, *Angew. Chem. Int. Ed.* **2017**, *56*, 15886–15890; *Angew. Chem.* **2017**, *129*, 16102–16106; d) S. Du, J. Yang, J. Hu, Z. Chai, G. Luo, Y. Luo, W.-X. Zhang, Z. Xi, *J. Am. Chem. Soc.* **2019**, *141*, 6843–6847.
[10] R. S. P. Turbervill, J. M. Goicoechea, *Chem. Commun.* **2012**, *48*, 6100–6102.
[11] A. J. Ashe, S. Mahmoud, C. Elschenbroich, M. Wünsch, *Angew. Chem. Int. Ed. Engl.* **1987**, *26*, 229–230; *Angew. Chem.* **1987**, *99*, 249–250.
[12] O. J. Scherer, C. Blath, G. Wolmershäuser, *J. Organomet. Chem.* **1990**, *387*, C21-C24.
[13] O. J. Scherer, T. Brück, *Angew. Chem. Int. Ed. Engl.* **1987**, *26*, 59; *Angew. Chem.* **1987**, *99*, 59.

[14] a) M. V. Butovskiy, G. Balázs, M. Bodensteiner, E. V. Peresypkina, A. V. Virovets, J. Sutter, M. Scheer, *Angew. Chem. Int. Ed.* **2013**, *52*, 2972–2976; *Angew. Chem.* **2013**, *125*, 3045–3049; b) M. Schmidt, D. Konieczny, E. V. Peresypkina, A. V. Virovets, G. Balázs, M. Bodensteiner, F. Riedlberger, H. Krauss, M. Scheer, *Angew. Chem. Int. Ed.* **2017**, *56*, 7307–7311; *Angew. Chem.* **2017**, *129*, 7413–7417.
[15] M. Piesch, M. Seidl, M. Scheer, *Chem. Sci.* **2020**, *11*, 6745–6751.
[16] E. Mädl, G. Balázs, E. V. Peresypkina, M. Scheer, *Angew. Chem. Int. Ed.* **2016**, *55*, 7702–7707; *Angew. Chem.* **2016**, *128*, 7833–7838.
[17] L. Dütsch, M. Fleischmann, S. Welsch, G. Balázs, W. Kremer, M. Scheer, *Angew. Chem. Int. Ed.* **2018**, *57*, 3256–3261; *Angew. Chem.* **2018**, *130*, 3311–3317.
[18] M. Fleischmann, F. Dielmann, G. Balázs, M. Scheer, *Chem. Eur. J.* **2016**, *22*, 15248–15251.
[19] M. Piesch, C. Graßl, M. Scheer, *Angew. Chem. Int. Ed.* **2020**, *59*, 7154–7160; *Angew. Chem.* **2020**, *132*, 7220–7227.
[20] M. Piesch, F. Dielmann, S. Reichl, M. Scheer, *Chem. Eur. J.* **2020**, *26*, 1518–1524.
[21] M. Piesch, M. Scheer, *Organometallics* **2020**, *39*, 4247–4252.
[22] P. Pyykkö, M. Atsumi, *Chem. Eur. J.* **2009**, *15*, 12770–12779.
[23] P. Pyykkö, M. Atsumi, *Chem. Eur. J.* **2009**, *15*, 186–197.
[24] M. Scheer, L. J. Gregoriades, A. V. Virovets, W. Kunz, R. Neueder, I. Krossing, *Angew. Chem. Int. Ed.* **2006**, *45*, 5689–5693; *Angew. Chem.* **2006**, *118*, 5818–5822.
[25] M. Fleischmann, S. Welsch, H. Krauss, M. Schmidt, M. Bodensteiner, E. V. Peresypkina, M. Sierka, C. Gröger, M. Scheer, *Chem. Eur. J.* **2014**, *20*, 3759–3768.
[26] a) A. R. Kudinov, D. A. Loginov, Z. A. Starikova, P. V. Petrovskii, M. Corsini, P. Zanello, *Eur. J. Inorg. Chem.* **2002**, *2002*, 3018–3027; b) O. J. Scherer, T. Brück, G. Wolmershäuser, *Chem. Ber.* **1989**, *122*, 2049–2054; c) M. Schmidt, A. E. Seitz, M. Eckhardt, G. Balázs, E. V. Peresypkina, A. V. Virovets, F. Riedlberger, M. Bodensteiner, E. M. Zolnhofer, K. Meyer et al., *J. Am. Chem. Soc.* **2017**, *139*, 13981–13984.
[27] O. J. Scherer, K. Pfeiffer, G. Heckmann, G. Wolmershäuser, *J. Organomet. Chem.* **1992**, *425*, 141–149.
[28] M. Scheer, C. Riesinger, L. Duetsch, G. Balazs, M. Bodensteiner, *Chem. Eur. J.* **2020**.
[29] S. Alvarez, *Dalton Trans.* **2013**, *42*, 8617–8636.
[30] F. Dielmann, A. Timoshkin, M. Piesch, G. Balázs, M. Scheer, *Angew. Chem. Int. Ed.* **2017**, *56*, 1671–1675; *Angew. Chem.* **2017**, *129*, 1693–1698.
[31] H. Sitzmann, G. Wolmershäuser, *Z. Naturforsch. B* **1995**, *50*, 750–756.
[32] J.-M. Lalancette, G. Rollin, P. Dumas, *Can. J. Chem.* **1972**, *50*, 3058–3062.
[33] T. Köchner, N. Trapp, T. A. Engesser, A. J. Lehner, C. Röhr, S. Riedel, C. Knapp, H. Scherer, I. Krossing, *Angew. Chem. Int. Ed.* **2011**, *50*, 11253–11256; *Angew. Chem.* **2011**, *123*, 11449–11452.
[34] M. Elsayed Moussa, M. Piesch, M. Fleischmann, A. Schreiner, M. Seidl, M. Scheer, *Dalton Trans.* **2018**, *47*, 16031–16035.
[35] O. J. Scherer, T. Dave, J. Braun, G. Wolmershäuser, *J. Organomet. Chem.* **1988**, *350*, C20-C24.
[36] J. J. Schneider, D. Wolf, C. Janiak, O. Heinemann, J. Rust, C. Krüger, *Chem. Eur. J.* **1998**, *4*, 1982–1991.

Manuscript received: March 7, 2021
Accepted manuscript online: April 15, 2021
Version of record online: ■■, ■■■

FULL PAPER

The redox chemistry of heterobimetallic triple-decker complexes (Fe/Co and Co/Ni) with polypnictogen ligands (E = P, As) was studied first by cyclic voltammetry and then experimentally. The complexes respond to the addition and withdrawal of electrons either by the rearrangement of the triple-decker geometry, by the fragmentation of the E_n ligand and/or by the exchange of {Cp‴M} fragments.

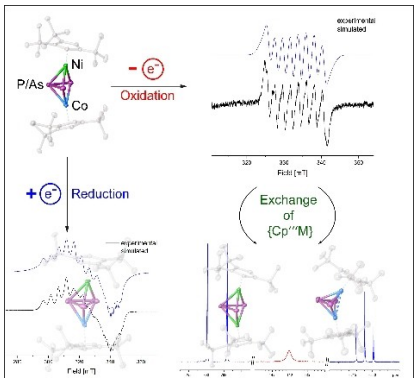

*Dr. M. Piesch, S. Reichl, C. Riesinger, Dr. M. Seidl, Dr. G. Balazs, Prof. Dr. M. Scheer**